J Therm Anal Calorim (2015) 119:213–218
DOI 10.1007/s10973-014-4138-z

Thermal analysis of quaternary *Ge–Se–Sb–Te* chalcogenide alloys

Neha Sharma · Sunanda Sharda · Vineet Sharma · Pankaj Sharma

Received: 4 June 2014 / Accepted: 26 August 2014 / Published online: 12 September 2014

Abstract *Tellurium*-based glasses are suitable for storage devices due to their rapid amorphous-to-crystalline transformation. Alloys of $Ge_{19-y}Se_{63.8}Sb_{17.2}Te_y$ ($y = 0$, 2, 4, 6, 8, 10 at.%) have been synthesized using melt quench technique. Glass transition and crystallization kinetics of alloys have been investigated using differential thermal analysis at different heating rates (5, 10, 15, and 20 K min^{-1}). The thermal stability of synthesized alloys has been investigated. Resistance to devitrification has been analyzed on the basis of activation energy for crystallization.

Keywords Chalcogenides · Non-crystalline materials · Thermodynamic properties

Introduction

Chalcogenides glasses are considered as functional materials due to their wide range of technological and scientific applications. There is an increased interest in chalcogenides due to their applications in infrared optical fibers in the field of environment science, materials science, and medical science [1–3]. One of the most promising applications of chalcogenide glasses is in phase-change memories [4]. The phase-change materials are designed due to the existence of two structural forms, amorphous and crystalline [5]. These glasses are useful for rewritable optical recording due to their reversible switching behavior between the amorphous and crystalline phase [4]. The amorphous state is metastable which inherently have a tendency to relax toward the equilibrium. These states have the possibility to transform into more stable crystalline state [6].

Ge−Se−Sb glasses have low transmission loss and high transparency in infrared (IR) region from 2 to 14 μm which makes them suitable in optical fibers [7]. We have already reported the ternary system, $Ge_{19}Se_{81-x}Sb_x$ for their physical, structural, optical, and thermal properties [7–10]. The study of reported properties indicates that the glass transition temperature is maximum and optical energy gap is minimum for $Ge_{19}Se_{63.8}Sb_{17.2}$ composition. *Te*-based glasses are used in optical memory devices such as rewritable digital versatile disks [11]. For the next generation of electronic non-volatile memories, these glasses are considered as the leading candidates [5]. We have already reported the physical and optical properties for $Ge_{19-y}Se_{63.8}Sb_{17.2}Te_y$ ($y = 0$, 2, 4, 6, 8, 10 at.%) alloys [12, 13]. Therefore, Te-alloyed $Ge_{19}Se_{63.8}Sb_{17.2}$ samples have been studied for thermal stability, glass and crystallization kinetics.

In the present communication, we report the thermal stability and glass forming ability of $Ge_{19-y}Se_{63.8}Sb_{17.2}Te_y$ alloys using differential thermal analysis (DTA). Three characteristic temperatures viz. glass transition temperature (T_g), crystallization temperature (T_c), and melting temperature (T_m) at different heating rates ($\alpha = 5$, 10, 15, 20 K min^{-1}) have been used to determine the activation energy for glass transition and crystallization [14–22]. For DTA study, non-isothermal method has been used due to

N. Sharma · V. Sharma · P. Sharma (✉)
Department of Physics and Materials Science, Jaypee University of Information Technology, Waknaghat, Solan 173234, H.P, India
e-mail: pks_phy@yahoo.co.in; pankaj.sharma@juit.ac.in

N. Sharma
Department of Physics, MCM DAV College, Kangra 176001, HP, India

S. Sharda
Department of Physics, IEC University, Baddi, Solan 174103, H.P, India

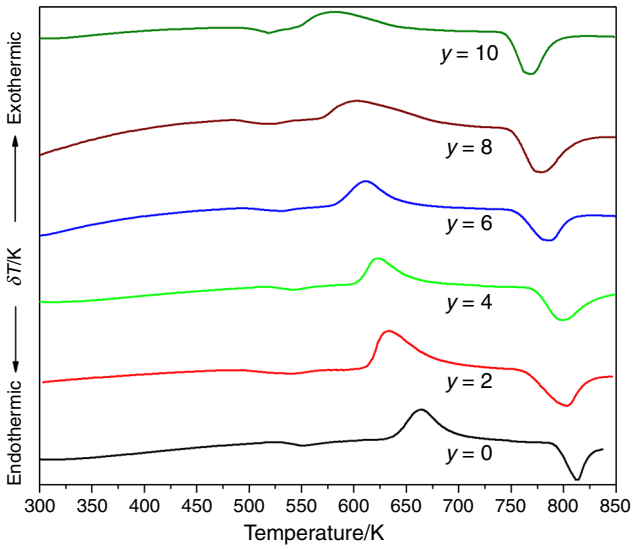

Fig. 1 DTA trace for $Ge_{19-y}Se_{63.8}Sb_{17.2}Te_y$ ($y = 0$, 2, 4, 6, 8, 10 at.%) alloys at heating rate 10 K min^{-1}

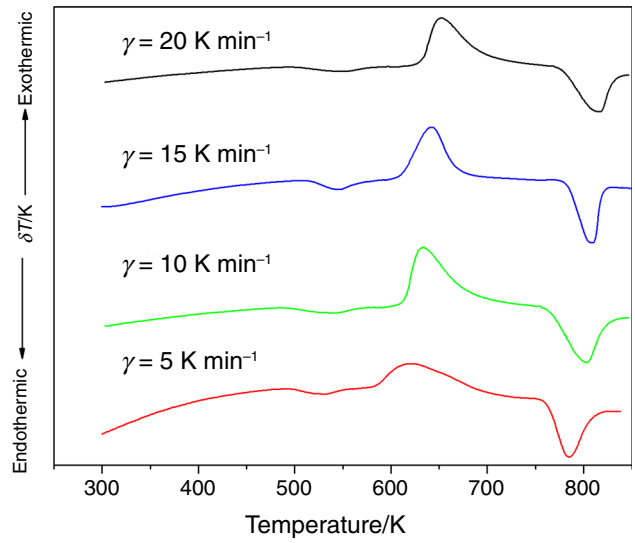

Fig. 2 DTA trace for $Ge_{17}Se_{63.8}Sb_{17.2}Te_2$ alloys at heating rate of 5, 10, 15 and 20 K min^{-1}

its applicability on a wide range of temperature and quick analysis in shorter time period [23].

Experimental

Melt quench technique has been used for alloy preparation of $Ge_{19-y}Se_{63.8}Sb_{17.2}Te_y$ ($y = 0$, 2, 4, 6, 8, 10 at.%) samples. The details of alloy synthesis have been reported elsewhere [7, 13]. X-ray diffraction spectra of bulk samples have been obtained from X-ray diffractometer [X'Pert Pro]. The absence of any prominent peak in spectra reveals the amorphous nature of the bulk samples (figure not shown here). The freshly prepared materials have been ground to fine powder and taken in the alumina pan for the DTA studies (EXSTAR TG/DTA 6300). For each DTA scan, 10 mg of powder has been used with different heating rates 5, 10, 15, and 20 K min^{-1}. The melting temperature and melting enthalpy of high purity indium, zinc, and lead have been used to calibrate the instrument, and the measurements have been carried out in nitrogen atmosphere at a flow rate of 200 mL min^{-1}. All the measurements have been carried under non-isothermal conditions.

Results and discussion

Three characteristic temperatures

DTA curves for $Ge_{19-y}Se_{63.8}Sb_{17.2}Te_y$ ($y = 0$, 2, 4, 6, 8, 10 at.%) alloys recorded at the heating rate of 5, 10, 15, and

Table 1 The values of glass transition temperature (T_g), crystallization temperature (T_c), and melting temperature (T_m) for $Ge_{19-y}Se_{63.8}Sb_{17.2}Te_y$ ($y = 0$, 2, 4, 6, 8, 10) glassy alloys at different heating rates (α)

Sample	α/K min^{-1}	T_g/K	T_c/K	T_m/K
$y = 0$	5	537.00	649.00	798.00
	10	546.00	663.72	812.00
	15	551.81	672.25	815.00
	20	555.44	679.18	821.00
$y = 2$	5	532.89	620.58	785.00
	10	542.00	633.96	803.10
	15	547.42	643.00	810.00
	20	552.00	652.00	817.32
$y = 4$	5	527.84	609.55	779.00
	10	536.89	622.00	796.00
	15	542.54	631.34	800.65
	20	547.57	640.97	807.12
$y = 6$	5	522.47	592.24	769.00
	10	530.18	612.00	787.00
	15	536.23	621.54	793.34
	20	542.00	629.97	800.00
$y = 8$	5	514.03	585.85	758.16
	10	522.34	602.01	778.97
	15	529.00	610.57	787.00
	20	534.00	617.91	796.00
$y = 10$	5	506.04	571.29	746.00
	10	516.71	582.18	768.94
	15	521.00	592.94	775.78
	20	527.00	602.69	784.00

20 K min^{-1} and are shown in Fig. 1 as reference at 10 K min^{-1}. Figure 2 shows DTA curves for $Ge_{17}Se_{63.8}Sb_{17.2}Te_2$ at the heating rate of 5, 10, 15, and 20 K min^{-1}. The characteristic features of these curves are glass transition temperature (T_g), crystallization temperature (T_c), and the melting temperature (T_m). The curve indicates an endothermic step at glass transition temperature, and the second peak is exothermic that takes place due to phase change. At this temperature, amorphous material begins to crystallize and is referred to crystallization temperature. The third peak is an endothermic peak which corresponds to melting temperature. The values of T_g, T_c, and T_m (Table 1) have been found to decrease with increasing content of *Te*.

Thermal stability and glass forming ability

Thermal stability is an important parameter for the analysis of glasses. Two criteria have been used to measure the thermal stability of glasses. The first criterion makes the use of difference between T_g and T_c [24]. The second criterion is Hruby parameter which indicates the glass forming ability (K_{gl}) [25, 26] and is expressed as

$$K_{gl} = \frac{T_c - T_g}{T_m - T_c}, \quad (1)$$

where $T_c - T_g$ represents the nucleation process and $T_m - T_c$ indicates the growth process. Kauzmann proposed the reduced glass transition temperature (T_{rg}) which is based on the theoretical relation between T_g and T_m and can be calculated as [26, 27]

$$T_{rg} = \frac{T_g}{T_m}. \quad (2)$$

According to the relation, T_{rg} should be constant and nearly equal to 2/3 for glasses. This relation is also called as two-thirds rule. It has been observed that the obtained values for T_{rg} obey the two-thirds rule (Table 2) and indicates the ease of glass formation for all the samples. Larger difference between T_c and T_g indicates that the kinetic resistance toward the crystallization is higher or vice versa. The glasses that show the crystallization peak near the glass transition temperature are considered as unstable glasses while the glasses having peak near the melting temperature are regarded as stable glasses. The difference between T_c and T_g values decreases with the addition of *Te* content indicating that the thermal stability parameter (K_{gl}) decreases. This indicates the decrease in thermal stability and hence the glass forming ability on addition of Te.

Table 2 Values of *A* and *B* for $Ge_{19-y}Se_{63.8}Sb_{17.2}Te_y$ ($y = 0, 2, 4, 6, 8, 10$) glassy alloys

Sample	*A*	*B*	K_{gl}	T_{rg}
$y = 0$	515.40	13.38	0.794	0.672
$y = 2$	510.63	13.74	0.544	0.674
$y = 4$	504.94	14.05	0.489	0.674
$y = 6$	499.20	13.97	0.468	0.674
$y = 8$	490.41	14.32	0.450	0.671
$y = 10$	482.50	14.64	0.351	0.672

The characteristic parameters K_{gl} and T_{rg} at $\alpha = 10$ K min^{-1}

Glass transition activation energy

The heating rate dependence of the glass transition temperature has been interpreted using an empirical relation [25, 28];

$$T_g = A + B\ln(\alpha), \quad (3)$$

where *A* and *B* are constants and α is the heating rate for the investigated samples. The plot between ln (α) and T_g (Fig. 3) gives the values of *A* and *B*. The value of *B* depends upon the cooling rate used during the preparation of samples [29], and it decreases with the decreasing cooling rate. The values of *A* have been observed to decreases with increasing content of *Te* (Table 2).

The glass transition activation energy (E_g) has been analyzed using two approaches. First approach uses the Kissinger formula for the analysis of dependence of T_g on the heating rate following the equation [14–17];

$$\ln\left(\frac{\alpha}{T_g^2}\right) = -\frac{E_g}{RT_g} + \text{const.}, \quad (4)$$

where *R* is gas constant and α the heating rate. The plot of $ln\ (\alpha/T_g^2)$ against $1{,}000/T_g$ yields a straight line whose slope gives the value of E_g (Fig. 4).

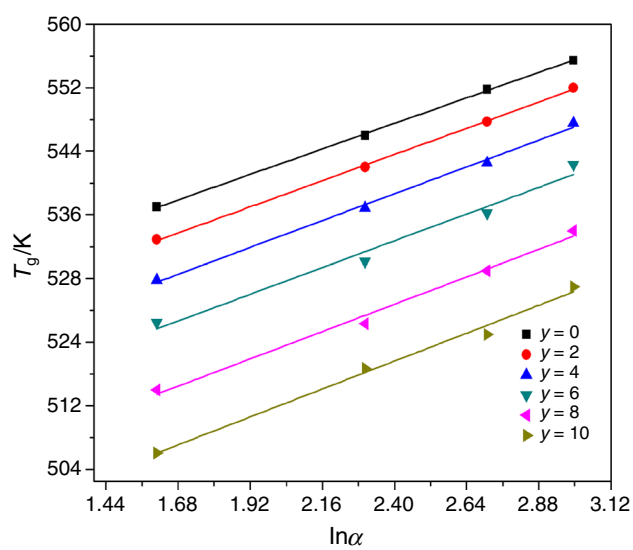

Fig. 3 Plot of T_g versus ln(α) for $Ge_{19-y}Se_{63.8}Sb_{17.2}Te_y$ ($y = 0, 2, 4, 6, 8, 10$ at.%) glasses

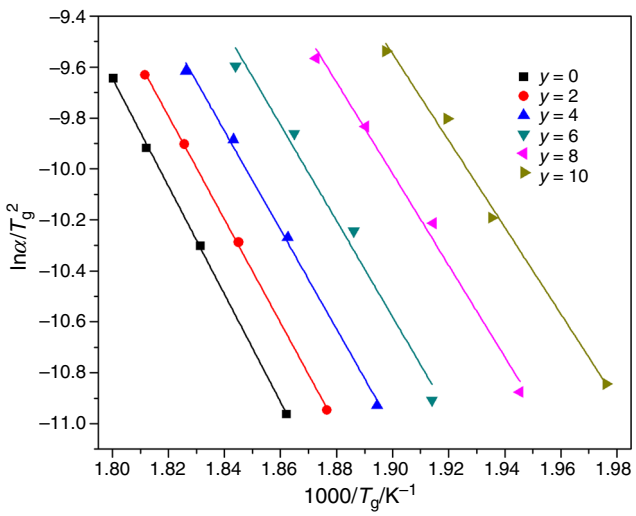

Fig. 4 Plot of $\ln(\alpha/T_g^2)$ versus 1,000/T_g for $Ge_{19-y}Se_{63.8}Sb_{17.2}Te_y$ ($y = 0, 2, 4, 6, 8, 10$ at.%) alloys

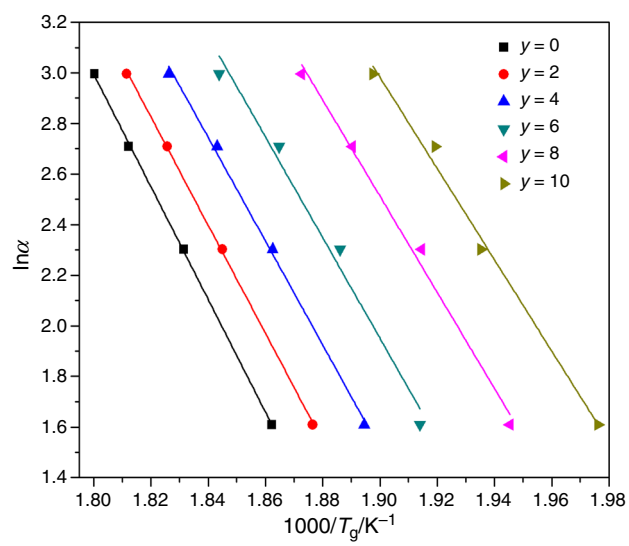

Fig. 5 Variation of ln(α) versus 1,000/T_g for the $Ge_{19-y}Se_{63.8}Sb_{17.2}Te_y$ ($y = 0, 2, 4, 6, 8, 10$ at.%) glasses

Moynihan and co-workers have developed the theory of structural relaxation based on the heating rate dependence of T_g to evaluate E_g [18, 19].

$$\frac{d(\ln \alpha)}{d(1/T_g)} = \frac{-E_g}{R}. \quad (5)$$

The plot of ln (α) versus 1,000/T_g has been used to determine the values of E_g (Fig. 5). The values of E_g decrease with addition of *Te* content (Table 3). The values obtained from these two methods are in good agreement with each other. In glass transition region, the energy needed to cross the energy barriers between metastable energy states is the activation energy of glass transition. Glasses with the minimum activation energy can cross the energy barrier more easily and hence, are stable. With the addition of *Te* content, the value of E_g decreases and the atoms of glasses have more probability to jump these metastable states.

Activation energy for crystallization

The activation energy for crystallization has been determined using two approximations [20–22]. The first approximation is based on the method given by Augis and Bennett, which follows the equation [20, 22]:

$$\ln(\alpha/T_c) = -E_c/RT_c + \ln K_o, \quad (6)$$

where K_o is pre-exponential factor indicating the number of attempts performed to overcome the energy barrier. The slope of the straight line between $\ln(\alpha/T_c)$ and temperature (Fig. 6) gives the value of E_c.

The activation energy for crystallization has been evaluated using the variation of T_c with α. Mahadevan et al. have approximated the Kissinger method for the analysis of devitrification process [21, 22]:

$$\ln(\alpha) = -\frac{E_c}{RT_c} + \text{const.} \quad (7)$$

The plot of $\ln(\alpha)$ versus 1,000/T_c gives straight line and hence, the values of activation energy have been calculated

Table 3 Values of glass transition activation energy (E_g), crystallization activation energy (E_c), and cohesive energy (*CE*) for $Ge_{19-y}Se_{63.8}Sb_{17.2}Te_y$ ($y = 0, 2, 4, 6, 8, 10$ at.%) glassy alloys

Sample	E_g (Kissinger)/kJ mol^{-1}	E_g (Moynihan)/kJ mol^{-1}	E_c (Augis and Bennett)/kJ mol^{-1}	E_c (Mahadevan)/kJ mol^{-1}	*CE*/kJ mol^{-1}
$y = 0$	176.22	185.29	163.82	169.31	197.34
$y = 2$	168.81	177.88	144.93	150.23	195.96
$y = 4$	161.57	170.56	139.44	144.61	194.58
$y = 6$	156.67	165.57	132.87	138.03	193.16
$y = 8$	149.43	158.08	126.05	131.04	191.78
$y = 10$	141.52	150.09	120.47	125.38	190.36

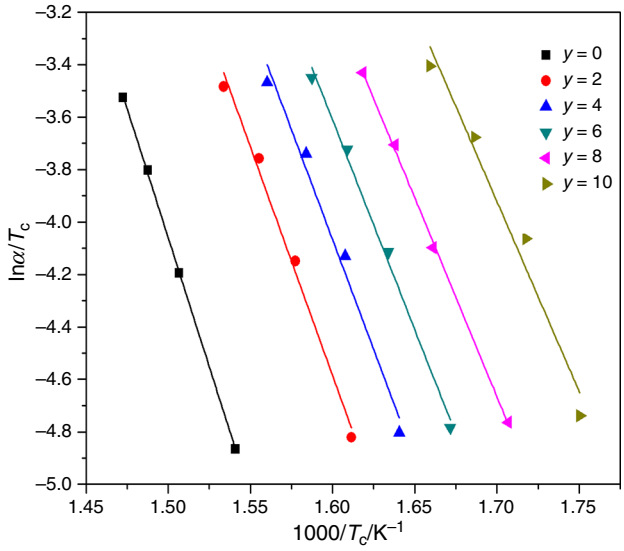

Fig. 6 Variation of $\ln(\alpha/T_c)$ versus $1{,}000/T_c$ for $Ge_{19-y}Se_{63.8}Sb_{17.2}Te_y$ ($y = 0, 2, 4, 6, 8, 10$ at.%) alloys

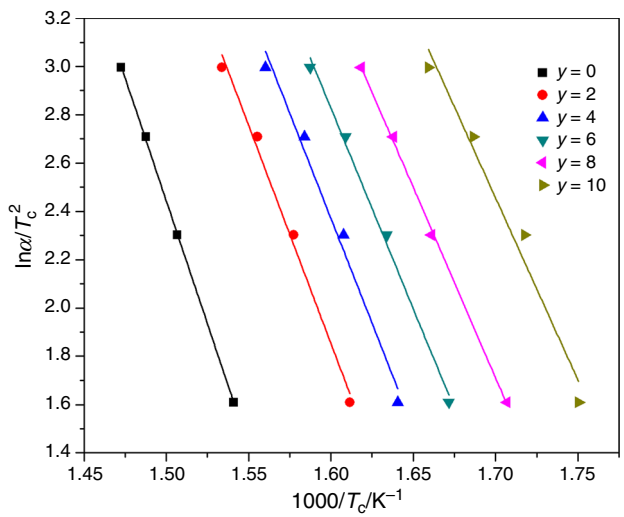

Fig. 7 Plot of $\ln(\alpha)$ versus $1{,}000/T_c$ for $Ge_{19-y}Se_{63.8}Sb_{17.2}Te_y$ ($y = 0, 2, 4, 6, 8, 10$ at.%) glassy alloys

from the slope (Fig. 7). The values of activation energy for crystallization (E_c) calculated from both the methods are in good agreement.

The activation energy for crystallization during the phase transformation decreases with the increasing content of *Te* (Table 3) and can be explained on the basis of cohesive energy (*CE*). The *CE* can be evaluated from the distribution of probable chemical bonds. The bond energy of *Ge*−*Se* is high and they are formed first, followed by *Te*−*Se* and *Sb–Se* bonds with slightly lower energy and then unsaturated *Se*−*Se* bonds are formed [12]. When *Ge* is replaced with *Te,* the probability of *Ge*−*Se* bond formation decreases leading to an increase in *Te*−*Se* bonds along with the formation of low-energy homopolar bonds. The cohesive energy of the system decreases with *Te* addition (Table 3). The decrease in E_c may be related to the nucleation and growth processes in which devitrification requires less energy as the value of *CE* decreases for the glassy network. This indicates that the probability of the system toward devitrification increases on Te alloying.

Conclusions

Thermal parameters T_g, T_c, and T_m have been calculated for $Ge_{19-y}Se_{63.8}Sb_{17.2}Te_y$ ($y = 0, 2, 4, 6, 8, 10$ at.%) glassy alloys. The values of the glass transition temperature and crystallization temperature increase with increasing heating rate but decrease with *Te* content. Glass forming ability decreases with increasing *Te* content. The glass transition activation energy decreases with addition of *Te* content. The tendency of the *Te* added system toward crystallization increases due to which the thermal stability decreases. The values of activation energy for crystallization can be explained using cohesive energy which decreases on addition of *Te*.

References

1. Redaelli A, Pirovano A. Nano-scaled chalcogenide-based memories. Nanotechnology. 2011;22(25):254021.
2. Lucas P, Solis MA, Coq DL, Juncker C, Riley MR, Collier J, Boesewetter DE, Boussard-Plédel C, Bureau B. Infrared biosensors using hydrophobic chalcogenide fibers sensitized with live cells. Sens Actuators B Chem. 2006;119(2):355–62.
3. Sharma A, Kumar H, Mehta N. Determination of specific heat in multi-component chalcogenide glasses of Se–Te–Sn–Pb system using modulated differential scanning Calorimetry. Mater Lett. 2012;86:54–7.
4. Al-Agel FA, Al-Arfaj EA, Al-Marzouki FM, Khan SA, Al-Ghamdi AA. Study of phase separation in $Ga_{25}Se_{75-x}Te_x$ chalcogenide thin films. Prog Nat Sci Mater Int. 2013;23:139–44.
5. Al-Agel FA. Crystallization kinetics and effect of thermal annealing on optical constants in a-$Ge_{25}Se_{75-x}Te_x$ glasses. J Alloy Compd. 2013;568:92–7.
6. Imran MM, Bhandari D, Saxena NS. Kinetic studies of bulk $Ge_{22}Se_{78-x}Bi_x$ (x = 0, 4 and 8) semiconducting glasses. J Therm Anal Calorim. 2001;65(1):257–74.
7. Sharma N, Sharda S, Sharma V, Sharma P. Far-infrared investigation of ternary Ge–Se–Sb and quaternary Ge–Se–Sb–Te chalcogenide glasses. J Non-Cryst Solids. 2013;375:114–8.
8. Sharma N, Sharda S, Sharma V, Sharma P. Structural Rigidity, Percolation and Transition-Temperature Study of the $Ge_{19}Se_{81-x}Sb_x$ System. Defect Diffus Forum. 2011;316:37–44.
9. Sharma N, Sharda S, Sharma V, Sharma P. Effect of antimony addition on thermal stability and crystallization kinetics of germanium–selenium alloys. J Non-Cryst Solids. 2013;371:1–5.
10. Sharma N, Sharda S, Sharma V, Sharma P. Optical analysis of $Ge_{19}Se_{81-x}Sb_x$ thin films using single transmission spectrum. Mater Chem Phys. 2012;136(2):967–72.

11. Siegel J, Schropp A, Solis J, Afonso CN, Wuttig M. Rewritable phase-change optical recording in $Ge_2Sb_2Te_5$ films induced by picosecond laser pulses. Appl Phys Lett. 2004;84(13):2250–2.
12. Sharma N, Sharda S, Sharma V, Sharma P. Evaluation of physical parameters for new quaternary $Ge_{19\text{-}y}Se_{63.8}Sb_{17.2}Te_y$ chalcogenide glasses. Chalcogenide Lett. 2012;9(8):355–63.
13. Sharma N, Sharda S, Katyal SC, Sharma V, Sharma P. Effect of Te on linear and non-linear optical properties of new quaternary Ge-Se-Sb-Te chalcogenide glasses. Electron Mater Lett. 2014; 10(1):101–6.
14. Kissinger HE. Variation of peak temperature with heating rate in differential thermal analysis. J Res Natl Bur Stand. 1956;57: 217–21.
15. Kissinger HE. Reaction kinetics in differential thermal analysis. Anal Chem. 1957;29:1702–6.
16. Colmenero J, Barandiaran JM. Crystallization of $Al_{23}Te_{77}$ glasses. J Non-Cryst Solids. 1978;30:263–71.
17. Shaaban ER, Tomash IBI. The effect of Sb content on glass-forming ability, the thermal stability and crystallization of Ge–Se chalcogenide glass. J Therm Anal Calorim. 2011;105:191–8.
18. Moynihan CT, Easteal AJ, Wilder J, Tucker J. Dependence of the glass transition temperature on heating and cooling rate. J Phys Chem. 1974;78(26):2673–7.
19. Patel AT, Pratap A. Study of kinetics of glass transition of metallic glasses. J Therm Anal Calorim. 2012;110:567–71.
20. Augis JA, Bennett JE. Calculation of the Avrami parameters for heterogeneous solid state reactions using a modification of the Kissinger method. J Therm Anal Calorim. 1978;13(2):283–92.
21. Mahadevan S, Giridhar A, Singh AK. Calorimetric measurements on As-Sb-Se glasses. J Non-Cryst Solids. 1986;88(1):11–34.
22. Sharda S, Sharma N, Sharma V, Sharma P. Glass transition and crystallization kinetics analysis of Sb–Se–Ge chalcogenide glasses. J Therm Anal Calorim. 2014;115:361–2.
23. Vázquez J, González-Palma R, Cárdenas-Leal JL, Barreda DGG, López-Alemany PL, Villares P. On the glass–crystal transformation kinetics in materials which fulfil the conditions of "site saturation". Application to the crystallization of some alloys of Sb–As–Se and Ge–Sb–Se glassy systems. J Mater Sci. 2010;45(11):2974–82.
24. Hrubý A. Evaluation of glass-forming tendency by means of DTA. Czechoslov J Phys B. 1972;22(11):1187–93.
25. Kumar R, Sharma P, Barman PB, Sharma V, Katyal SC, Rangra VS. Thermal stability and crystallization kinetics of Se–Te–Sn alloys using differential scanning calorimetry. J Therm Anal Calorim. 2012;110(3):1053–60.
26. Naqvi SF, Saxena NS. Kinetics of phase transition and thermal stability in $Se_{80\text{-}x}$–Te_{20}–Zn_x ($x = 2, 4, 6, 8, 10$). J Therm Anal Calorim. 2012;110(3):1053–60.
27. Kauzmann W. The nature of the glassy state and the behavior of liquids at low temperatures. Chem Rev. 1948;43:219–56.
28. Heireche MM, Belhadji M, Hakiki NE. Non–isothermal crystallization kinetics study on Se_{90-x}–In_{10}–Sb_x ($x = 0, 1, 2, 4, 5$) chalcogenide glasses. J Therm Anal Calorim. 2013;114:195–203.
29. Calventus Y, Surinach S, Baro MD. Thermal stability and crystallization kinetics study of some Se–Te–Ge glassy alloys. Mater Sci Eng A. 1997;226:818–22.